A Single-Phase Induction Machine Model for Real-Time Digital Simulation

A. B. Dehkordi

***Abstract*— Most small power induction motors need to operate with single-phase a.c. power supplies that are readily available at homes, and remote rural areas [1]. These machine are used to drive fans, pumps, air compressors, refrigeration compressors, air conditioning fans and blowers, saws, grinders and office machines [2].**

This paper presents a real-time electromagnetic transient model for single-phase induction machines (SPIM). The paper starts with the introduction and analysis of unsymmetrical 2-phase induction machines. Although, main and auxiliary windings are not symmetric, a technique has been introduced which facilitates the inclusion of magnetic saturation in this model. The embedded phase domain approach [3] is utilized for incorporation of this model into the network solution of the RTDS™ simulator. Various features of the model such as embedded breakers are introduced in the paper. The model is validated using stand-alone numerical simulations and analytical solutions. Possible configurations of the model such as "capacitor-start induction motor" and "capacitor-start capacitor-run induction motor", are demonstrated. Scenarios including stalling of air-conditioning pumps during a fault in distribution circuits are presented.

***Keywords*: real-time digital simulation, single-phase induction machine, saturation, embedded phase domain approach, digital transient network analyzer, distribution network**

I. Introduction

Small power motors in distribution networks normally have to operate with single-phase a.c. power. These machines are either series connected d.c. machines or single-phase induction machines (SPIMs). Single-phase induction machines are used to drive fans, pumps, air compressors, refrigeration compressors, air conditioning fans and blowers, saws, grinders and office machines [2]. Air conditioning systems used in households generally include a condenser unit, a compressor unit and an air handler fan. Both the compressor unit and the fan are run by single-phase induction motors.

To be self-starting, the induction machine needs a rotating field at zero speed. This in turn implies the presence of two windings in the stator, while the rotor has a standard squirrel cage [1]. The stator first winding is called the main winding whereas the second winding is called the auxiliary winding [1]. SPIMs may run only on the main winding once they started on two windings. A typical case of single-phase single-winding IM occurs when a three-phase IM ends up with an open phase. The power factor and efficiency degrade while the peak torque also decreases significantly [1]. Thus, except for low powers (less than ¼ kW in general), the auxiliary winding is active also during running conditions to improve the performance. The following are the main types of single-phase induction motors in use today:

- Split-Phase Induction Motors
- Capacitor Induction Motors
- Shaded-Pole Induction Motors

The split-phase motor, sometimes called resistance split-phase, achieves its starting torque by having a higher resistance and possibly lower reactance in the auxiliary circuit, which is usually wound 90 electrical degrees from the main winding. At a speed in the region of maximum torque, the auxiliary winding is switched off. The switch may be activated by speed (centrifugal), voltage, current, or temperature [2]. The starting torque of these motors is moderate, but the starting current is relatively high. Efficiency and power factor are moderate, with efficiency ranging from about 40% at 0.1 hp to about 70% at 0.75 hp [1].

Capacitor induction motors are in the forms of "capacitor-start motors", "permanent-split capacitor motors" and "two value capacitor motors". In the "capacitor-start" motor the starting torque is obtained by the use of a capacitor in series with the auxiliary winding while starting, then switching the auxiliary winding out as the motor reaches running speed. The capacitor causes the auxiliary winding current to lead the main current. These machines are used for hard to start applications such as pumps, compressors, etc. up to the rating of 5 hp [2]. A permanent-split capacitor motor is designed for applications where starting torque requirements are low, but improved running performance is required. In this case, the motor is designed to have a capacitor in series with the auxiliary winding all the time [2].

In a "two-value capacitor motor", a start capacitor is placed in parallel with the run capacitor. This allows the motor to be designed for optimum running efficiency without sacrificing efficiency to get starting torque. Two-value capacitor motors have been available for years in the range of 1-10 hp [2].

In "shaded-pole machines", the auxiliary winding is usually a simple shorted turn of conductor around one side of each stator pole, called a shading coil. Shaded-pole motors are simple in construction and are therefore relatively low cost and reliable. Starting current is relatively high, starting torque is relatively low, running current is relatively high, and efficiency and power factor are low [2]. They are widely used to drive small fans (1/5 hp and below) because they are low in cost and reliable.

Electric utilities have been having occurrences of delayed

A. B. Dehkordi is with RTDS Technologies Inc., Winnipeg, Canada (e-mail: dehkordi@rtds.com).

Paper submitted to the International Conference on Power Systems Transients (IPST2015) in Cavtat, Croatia June 15-18, 2015.

voltage recovery following faults on the electrical system when the load is comprised largely of loads driven by induction machines. Under normal conditions, voltage recovers to nominal levels in less than one second after the fault is cleared. In several cases, voltage recovery has been delayed for over 30 seconds after normal fault clearing in some substations, especially when the air temperature and electrical system loading was high [5]. This fault induced delayed voltage recovery or FIDVR, is being attributed to stalling of air conditioner units. Mainly, stalling of the single-phase induction motor operating the compressor unit. Delayed voltage recovery may lead to a system voltage collapse in the worst case. One of the recent applications of the real-time simulators has been on the modeling of distribution circuits and interaction of air conditioning loads within these networks [6].

This paper presents development of a single-phase induction machine model (SPIM) for real-time digital simulation. The paper starts with the introduction and analysis of unsymmetrical 2-phase induction machines. Methods of transient simulation of single-phase induction machines are discussed. Although, the main and auxiliary windings are not symmetrical, a technique has been introduced which facilitates the inclusion of magnetic saturation in this model. The embedded phase domain approach [4] is utilized for incorporation of this model into the network solution of the simulation. Various features of the model such as embedded breakers are introduced in the paper. The model is validated using stand-alone numerical simulations and analytical solutions. Possible configurations of the model such as "capacitor-start induction motor" and "capacitor-start capacitor-run induction motor", are demonstrated. Examples, including stalling of air-conditioning pumps during a fault in distribution circuits, are presented.

II. Theory and Analysis of a SPIM

This section briefly describes the analysis and modeling method of single-phase induction machines. Since the goal is incorporation of the model into an electromagnetic transient program, the coupled electric circuit approach is used for the analysis of this electric machine. Some of the previous contributions [7]-[9] are outlined and techniques offered in this paper are described.

A. General Description of a Single-Phase Induction Machine

As mentioned above, a single-phase induction machine consists of two stator windings known as the main and auxiliary windings with the angular space of normally 90°. The stator windings are usually asymmetric, i.e. the main and auxiliary windings do not have the same number of turns and parameters. The rotor has the standard squirrel cage, which in rotating field theory can be represented by two d- and q-axis windings. Fig. 1 shows the diagram of an idealized two-phase induction machine. Windings *as* and *bs* represent stator windings and windings *ar* and *br* represent rotor windings. The rotor angle is shown by θ_r and rotor speed is shown by ω_r. In this analysis, stator phase *as* is the main winding of the machine and stator phase *bs* is the auxiliary winding. As previously mentioned, they are not identical and they do not have the same parameters. The ratio of effective turns between the auxiliary and main windings N_{bs}/N_{as} is usually shown by the symbol a. The rotor windings are symmetric and have similar parameters.

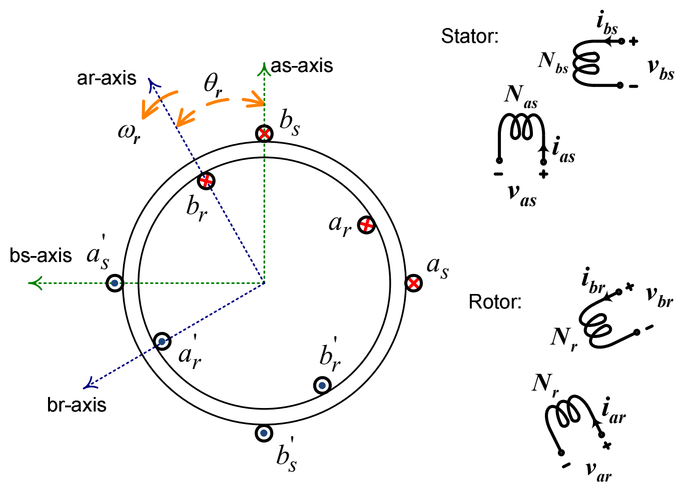

Fig. 1. Diagram of an idealized two-phase induction machine.

B. Voltage and Flux Linkage Equations and Equivalent Circuits

Based on the above description of a SPIM, voltage and flux linkage equations of a single-phase induction machine are developed. The following assumptions are made in this analysis:

- A multi-pole single-phase induction machine is modeled as an equivalent two pole machine. Torque and speed are monitored in p.u.
- It is assumed that the machine windings produce a sinusoidal MMF, thus space harmonics are ignored.

Voltage equations for a two-phase induction machine are presented in (1). Equation (1) shows the relation between voltage, current and flux linkage vectors of the machine. Stator phases *a* and *b* have different resistances due to the fact that stator windings are not symmetrical.

$$\overbrace{\begin{pmatrix} v_{as} \\ v_{bs} \end{pmatrix}}^{\underline{v}_{abs}} \atop \underbrace{\begin{pmatrix} v_{ar} \\ v_{br} \end{pmatrix}}_{\underline{v}_{abr}} = \left(\begin{matrix} \overbrace{\begin{bmatrix} r_{as} & 0 \\ 0 & r_{bs} \end{bmatrix}}^{[r_s]} & \begin{bmatrix} 0 & 0 \\ 0 & 0 \end{bmatrix} \\ \begin{bmatrix} 0 & 0 \\ 0 & 0 \end{bmatrix} & \underbrace{\begin{bmatrix} r_r & 0 \\ 0 & r_r \end{bmatrix}}_{[r_r]} \end{matrix} \right) \begin{matrix} \overbrace{\begin{pmatrix} i_{as} \\ i_{bs} \end{pmatrix}}^{\underline{i}_{abs}} \\ \underbrace{\begin{pmatrix} i_{ar} \\ i_{br} \end{pmatrix}}_{\underline{i}_{abr}} \end{matrix} + \frac{d}{dt} \begin{matrix} \overbrace{\begin{pmatrix} \Psi_{as} \\ \Psi_{bs} \end{pmatrix}}^{\underline{\Psi}_{abs}} \\ \underbrace{\begin{pmatrix} \Psi_{ar} \\ \Psi_{br} \end{pmatrix}}_{\underline{\Psi}_{abr}} \end{matrix} \qquad (1)$$

The relation between flux linkages and currents is shown in (2). Here, Ψ_{as} and Ψ_{bs} are flux linkages for stator windings a and b, and Ψ_{ar} and Ψ_{br} are flux linkages for rotor windings respectively. $[L_{ss}]$ and $[L_{rr}]$ are the inductance matrices for stator and rotor windings, and $[L_{sr}]$ is the matrix for the mutual inductances between the stator and rotor windings. The values of inductances in (2) are functions of rotor position and saturation.

$$\begin{pmatrix} \underline{\Psi}_{abs} \\ \underline{\Psi}_{abr} \end{pmatrix} = \begin{pmatrix} \left[L_{ss}\right] & \left[L_{sr}\right] \\ \left[L_{sr}\right]^T & \left[L_{rr}\right] \end{pmatrix} \begin{pmatrix} \underline{i}_{abs} \\ \underline{i}_{abr} \end{pmatrix} \text{ where:}$$

$$\left[L_{ss}\right] = \begin{bmatrix} L_{las} + L_{mas} & 0 \\ 0 & L_{lbs} + L_{mbs} \end{bmatrix}$$
$$\left[L_{rr}\right] = \begin{bmatrix} L_{lr} + L_{mr} & 0 \\ 0 & L_{lr} + L_{mr} \end{bmatrix} \quad (2)$$
$$\left[L_{sr}\right] = \begin{bmatrix} M_{ar}\cos(\theta_r) & -M_{ar}\sin(\theta_r) \\ M_{br}\sin(\theta_r) & M_{br}\cos(\theta_r) \end{bmatrix}$$

The voltage and flux linkage equations in (1) and (2) can be transferred to stator frame of reference so that the inductances no longer depend on the rotor position. With that, d- and q-axis equivalent circuits can be achieved. Note that, due to the asymmetry in stator windings, transforming the above equations to rotor frame of reference does not result in a position-independent inductance matrix [7]-[9].

In [8], q- and d-axis equivalent circuits are extracted with reference to main and auxiliary windings individually, thus the q- and d-axis magnetizing inductances are not equal. Fig. 2 shows the equivalent circuit of the machine using the approach used in [8]. It is usual to have SPIM data available in this form.

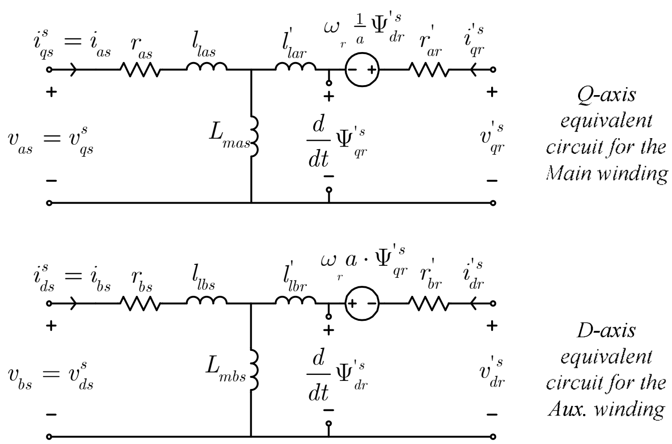

Fig. 2. Equivalent circuit of an idealized two-phase induction machine (rotor windings reflected to main and aux. windings).

III. Implementation of the SPIM Model into the Environment of the Real-Time Digital Simulator

The RTDS simulator is a combination of computer hardware and software designed specifically for the solution of power system electromagnetic transients in real time. Each unit of RTDS is called a rack. Every rack consists of processors dedicated to the solution of power system network, power system devices and control components [11]. Each simulation time-step is divided into computation intervals and communication intervals. Similar to other electromagnetic transient programs such as EMTP and EMTDC, Dommel algorithm [12] is used for discretization of the system's differential equation. Subsequently, nodal solution is used for calculation of node voltages. Differential equations of power system components are discretized to a Norton equivalent of conductances and current sources which are passed to the network solution during a communication interval (T_0) every time-step [11].

Interface vs Embedded Approach:

In electromagnetic transient programs, one approach of incorporating electric machines into the network solution is to consider a machine an *external sub-network* to the main system; receive the terminal voltages at every time-step and compute winding currents and inject them back to the network solution. This method is called *interfaced-based approach* [13], [14]. Another approach, referred to as the embedded approach, considers the machine as a set of mutually coupled inductances and applies precise implementation of Dommel algorithm to extract the discretized Norton equivalent of the machine model. This method is computationally more extensive than the interfaced-based approach as the time-varying inductance matrix of the machine needs to be inverted every time-step. Also, elements of the equivalent admittance matrix need to be sent to the network solution of the RTDS simulator every time-step. Details of implementing this method are discussed previously in [3], [4]. This approach provides a more numerically stable solution than the interfaced-based approach [3], [4]. This method also provides more flexibility in providing enhancements to the model such as inclusion of embedded breakers and arbitrary connection of the windings and nodes.

In this paper, the embedded phase-domain approach is used for incorporating the single-phase induction machine model into the network solution of RTDS: The trapezoidal rule of integration is directly applied to discretize the phase-domain differential equation of the SPIM described in (1) and (2). As SPIM inductances are changing with rotor position and magnetic saturation, equivalent conductance matrix and history terms are calculated and passed to the network solution of the simulator every each time-step.

The "CBuilder" utility of RSCAD software [11] is used for implementation of this model. This utility allows the user to implement a model in *C language* and creates a suitable assembly code for the target processor.

Inclusion of the effects of magnetic saturation:

Inclusion of magnetic saturation into the transient simulation of the SPIM model is one of the contributions of this paper. The rotor of a single-phase induction machine is round similar to that of a 3-phase induction machine. The air-gap is also uniform. This means that similar to a 3-phase induction machine, magnetic saturation can be included by adjusting the magnetizing inductance as a function of total magnetizing flux. However, as a SPIM has unsymmetrical stator windings (main and auxiliary), magnetizing inductance seen from the q- and d-axis L_{mq} and L_{md} are not equal. Numerical problems may arise if these magnetizing inductances are to be adjusted independently. Furthermore, in contrast to previous work [7]-[9], the implementation of this model is done in phase-domain, thus phase domain inductances need to be evaluated each time-step as a function of saturation.

The key factor in considering saturation is to observe the rotor in its natural state as a round rotor, i.e. having equal magnetizing inductances on both q- and d-axes. This can be done by observing all rotor and stator windings from the port of **one** of the stator windings e.g. stator main winding (see the equivalent circuit in Fig. 3.). This approach [9], reflects all of the windings to the main stator winding. Fig. 3 shows the equivalent circuit of the machine using this approach.

Usually, data for single-phase induction machines is available in both formats shown in Fig. 2 and Fig. 3. Parameters can be transferred from one circuit to another using the value of Aux. / Main turns ratio (a) and can be measured using standard no-load, locked-rotor and standstill frequency response tests [10]. In the model developed in this paper, the input data for the rotor is in the form of parameters in the equivalent circuit shown in Fig. 3. Therefore, only one value for rotor resistance and leakage inductance is required. If the available data is in the form of equivalent circuit shown in Fig. 2, then q-axis rotor resistance and leakage inductance is adequate for the model. D-axis rotor parameters are equal to q-axis parameters multiplied by (a^2). See [11] for more details.

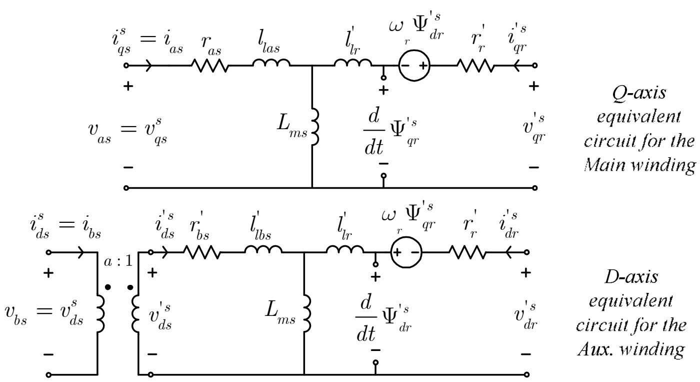

Fig. 3. Equivalent circuit of an idealized two-phase induction machine (all windings reflected to the main windings).

In every time-step, d- and q-axes magnetizing currents are calculated and from those the total magnetizing current $i_m = \sqrt{i_{md}^{\ 2} + i_{mq}^{\ 2}}$ is evaluated. Saturated magnetizing inductance L_{ms} is evaluated from the saturation curve and state of the magnetizing inductance. Then, saturated values of phase-domain inductances are evaluated from the saturated magnetizing inductance. Subsequently, a new inductance matrix is used in the embedded phase domain algorithm of the machine.

Torque and Mechanical Swing Equations:

The following set of equations is used for calculating electric torques and solving mechanical swing equations.

$$T_e = \frac{p}{2} \cdot L_{ms} \cdot \begin{pmatrix} i_{as} & i_{bs} \end{pmatrix} \begin{pmatrix} -\sin(\theta_r) & -\cos(\theta_r) \\ a \cdot \cos(\theta_r) & -a \cdot \sin(\theta_r) \end{pmatrix} \begin{pmatrix} i'_{ar} \\ i'_{br} \end{pmatrix} \qquad (3)$$

$$T_m(pu) - T_e(pu) = 2H \cdot \tfrac{d}{dt}\,\omega(pu) + D \cdot \omega(pu)$$

Features and Capabilities of the Model:

With the above description, the single-phase induction machine model is implemented in the environment of RTDS simulator. This section describes the capabilities of this model. The basic icon for this component appears as shown in Fig. 4. The terminals for stator main and auxiliary windings and the neutral point are respectively shown by M, A and N. Each of the main and auxiliary windings have embedded series breakers that can be controlled independently.

A capacitor, a resistor or a combination of resistive and capacitive elements can be inserted between nodes A and M, resulting in a capacitor-start, capacitor-run, two-value capacitor motor or other arrangements. Twelve instances of this model can be simulated in real-time using one PB5 processor [11] of the RTDS simulator.

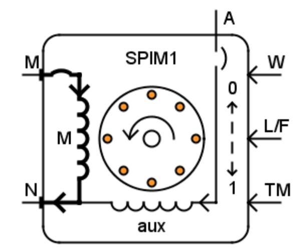

Fig. 4. The icon for RTDS single-phase induction machine model.

IV. Validation of the Model and Time-Domain Simulation Results

This section provides validations for the SPIM model presented in this paper. The focus of this section is to provide validations for the capability of the real-time model in accurately solving the differential equations of a single-phase induction machine stated in (1) and (2). Note that, these equations and the corresponding equivalent circuits are accepted forms for the SPIMs in the analysis of electric machinery [7]-[10].

The real-time simulation results are compared against the analytical solution of the model to provide validations in steady state performance of the model.

To validate the performance of the real-time model in transient conditions, a small off-line stand-alone electromagnetic transient program including a stand-alone SPIM model is developed. This tool allows lowering of the simulation time-step to values much lower than 50.0 μs (e.g. 1.0 μs) in order to obtain more accurate results. Magnetic saturation is also included in the off-line program. Note that, the inclusion of magnetic saturation into the analysis of SPIMs for electromagnetic transient programs is one of the contributions of this paper. Comparing the real-time simulation results against the results of the off-line program provides validations for the real-time model in transient conditions.

Signals labeled “RTDS” in this section and all the signals in Fig. 10 are real-time response from the model. Parameters for the SPIM under study are shown in the Appendix.

A. Comparison Against Analytical Solution

Using the revolving field theory and decomposing the rotating magnetic field into forward and backward fields, the steady state equivalent circuit of a single-phase induction machine [1], [2] and [15] can be extracted as shown in Fig. 5. Using this equivalent circuit, at standstill, the magnitude of the impedance seen from the main winding terminal is analytically calculated and compared against the numerical results from the real-time model. The results are shown in Fig. 6.

In another experiment, the magnitude of this impedance is calculated while the main winding is supplied with a 60*Hz* voltage source and the rotor speed is changed from -1.0 pu – 1.0 pu (slip = -2.0 – 0.0) . Analytical solution is compared against the simulation results in Fig. 7. As can be seen in both figures, simulation results and analytical solutions are identical. Note that in the above analysis, the auxiliary winding is open and saturation effects are ignored.

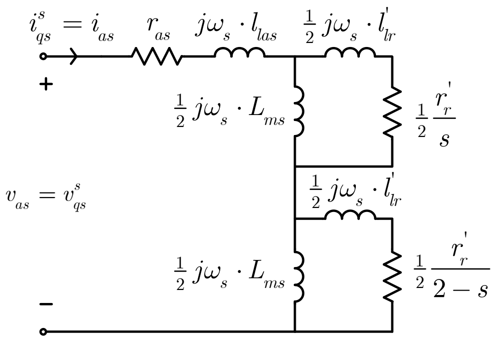

Fig. 5. Steady-state equivalent circuit of a single-phase induction machine.

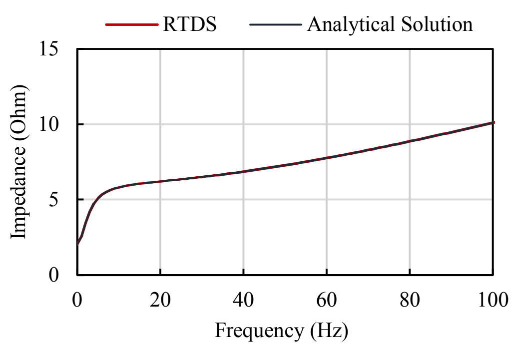

Fig. 6. Standstill frequency response of the SPIM from the port of main winding.

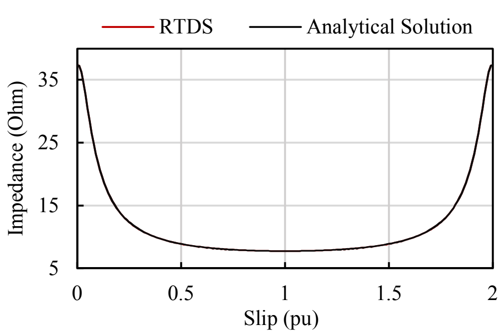

Fig. 7. Impedance vs slip characteristics of the SPIM

B. Comparison Against Stand-Alone Models

To validate the real-time model further, a stand-alone single-phase induction machine model is developed. The solution of this model is also in phase domain. In this experiment, the start-up of a SPIM from zero speed is simulated. During the start-up a constant mechanical torque of $1.0\ \mathrm{pu}$ is applied on the shaft.

The main and auxiliary windings are energized with $0.11\ kV\angle 0^\circ$ and $0.13\ kV\measuredangle -93^\circ$ 60 *Hz* voltage sources. During the start-up, once the machine speed reaches $0.8\ \mathrm{pu}$, the auxiliary winding breaker is opened which takes this winding out of circuit. This experiment is repeated with the real-time model and the results are compared in the following figures. Fig. 8a shows the stator main currents captured from the stand-alone offline simulation and the real-time model. Fig. 8b and Fig. 8c respectively show the start-up torque and speed signals from the above approaches. As can be seen, there is a very good agreement between the results of the stand-alone offline program and of the real-time model presented in this paper.

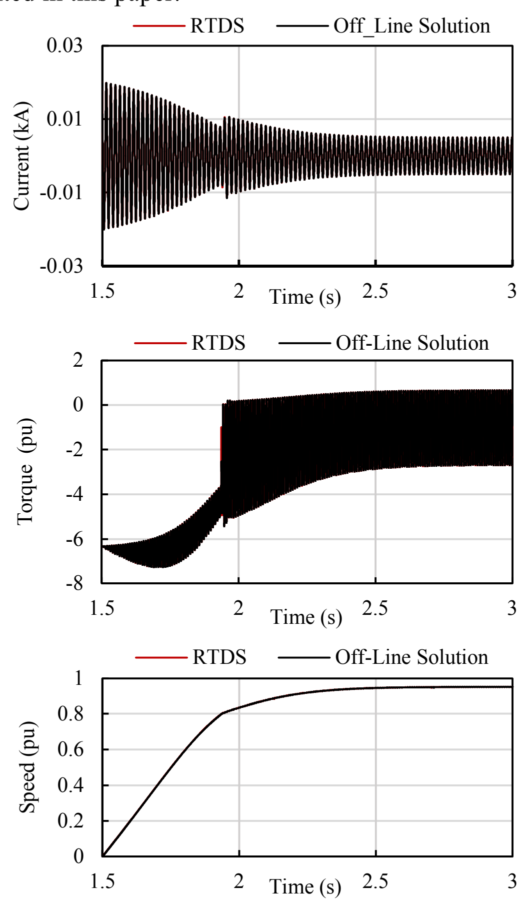

Fig. 8. Start-up of the SPIM. (a) Main winding current. (b) Electric torque. (c) Speed

V. EXAMPLE OF STALLING AIR-CONDITIONING COMPRESSOR UNITS AFTER A REMOTE FAULT

This section presents an example of SPIMs of the type typically used in air-conditioning units. The SPIMs stall after a fault. A small circuit containing two single-phase induction machines is simulated using the RTDS simulator. As shown in

Fig. 9, a permanent capacitor with the capacitance of 15.4 µF and resistance of 9.0 Ω is connected between the main and auxiliary terminals of the SPIMs. In this example, the auxiliary winding breaker is always closed. Induction machine parameters are shown in the Appendix. The mechanical load is based on the typical torque-speed characteristics of a centrifugal pump [16]. Both machines are supplied from a 0.11 *k*V, 60 *Hz* voltage source, representing one phase of a distribution system. In steady-state, a solid remote fault with the duration of 3 s is applied to the source. Fig. 10 shows the simulation results during this fault and after it is cleared. The voltage drop (Fig. 10a) during the fault reduces the SPIM electromagnetic torque significantly which in turn decreases rotor speed. Since the fault duration is long enough, speed signals for both SPIMs eventually reach zero causing stalling of the SPIMs and compressors (Fig. 10d). Once the fault is cleared, the voltages at the terminals of the SPIMs tend to recover. However, the SPIMs are still stalled and draw a large amount of current (Fig. 10b) which results in a large voltage drop across the series impedance of the source, causing terminal voltages not to recover fully. At this point, the electromagnetic torque produced by each SPIM is not large enough to surpass the minimum torque [16] required to rotate the stalled pump. This causes the SPIMs and compressors to stay stalled even after the fault is cleared (Fig. 10d). The SPIMs stay stalled until one of them is disconnected from the circuit. Another interesting observation in this experiment is the SPIM's loss during the fault. As can be seen in Fig. 10c, once a SPIM is stalled, most of the power absorbed by a machine is turned to resistive losses. This is consistent with the expected behavior of physical SPIMs in air-conditioning systems. This loss causes extra heat in the SPIMs and eventually thermal protection may isolate the machines from the circuit. Similar results are achieved when the fault is applied to the line.

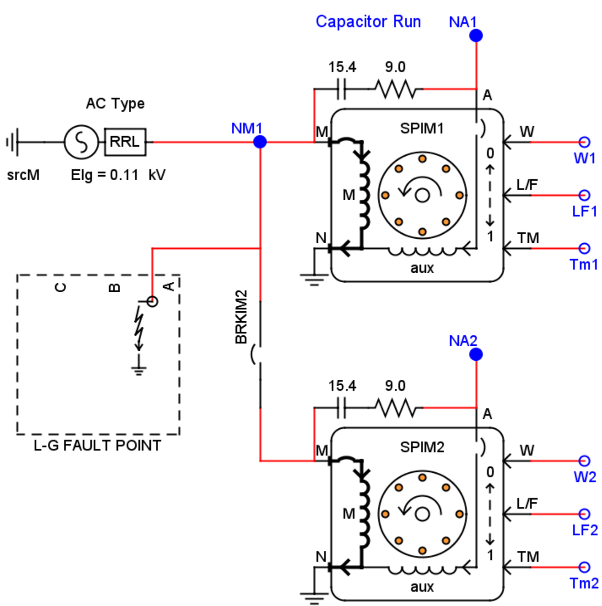

Fig. 9. Simulated circuit for stalling of SPIMs.

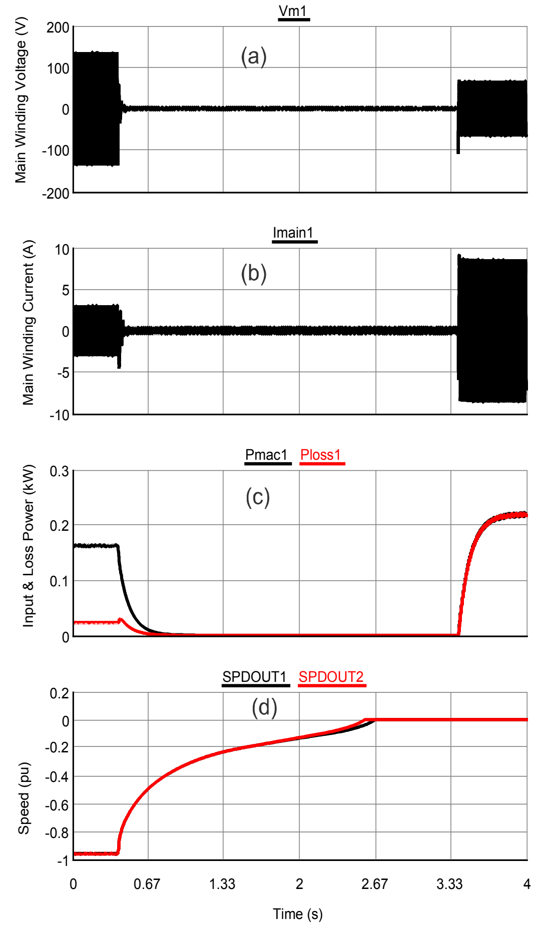

Fig. 10. SPIM signals during a remote fault.

VI. Conclusions

A detailed transient single-phase induction machine model was developed in this paper which is suitable for electromagnetic transient programs and real-time simulation. The model has the following important properties:

- The embedded phase domain approach [3], [4] is utilized for incorporation of this model into the network solution of the RTDS simulator.
- Magnetic saturation is included into the model by reflecting all the windings to the stator main winding and adjusting the magnetizing inductance according to the total magnetizing flux.

The model presented in this paper was validated using analytical solutions and stand-alone off-line simulations. Examples for applications of this model in simulating scenarios related to the stalling of air-conditioning pumps in distribution systems were presented. This detailed model can be used for a variety of studies in distribution networks. It also assists with the growing applications of electromagnetic transient programs and real-time simulators in studies related to distribution systems.

VII. Appendix

TABLE I
PARAMETERS OF THE SPIM [8]

Per-Unit Base	**Value**	
Line-neutral rated voltage	0.11 kV	
Rated MVA	0.186 kVA	
Rated Frequency	60 Hz	
Impedance base value	64.9 Ω	
Inductance base value	172.16 mH	
Aux. / main turn ratio	1.18	
Inertia Constant (H)	1.39 s	
Parameter Value	**Per-Unit**	**Physical**
Main winding resistance	0.031	2.02 Ω
Main winding leakage reactance	0.043	2.79 Ω
Unsaturated magnetizing reactance	1.029	66.8 Ω
Aux. winding resistance	0.11	7.14 Ω
Aux. winding leakage reactance	0.05	3.22 Ω
Rotor winding resistance	0.063	4.12 Ω
Rotor winding leakage reactance	0.033	2.12 Ω
Saturation Data		
Magnetizing Current (Norm)	Voltage (pu)	
0.0	0.0	
0.5	0.5	
0.8	0.79	
1.0	0.947	
1.2	1.076	
1.5	1.2	
1.8	1.3	
2.2	1.39	
3.2	1.58	
4.2	1.74	

VIII. Acknowledgment

The author sincerely appreciates the high valued technical support from the colleagues at RTDS Technologies Inc.

IX. References

[1] Ion Boldea, Syed A. Nasar, *The Induction Machine Handbook*, CRC Press LLC, 2002, Chapter 23.
[2] Hamid A. Toliyat, Gerald B. Kliman, *Handbook of Electric Motors*, CRC Press LLC, 2004, Chapter 2.
[3] A. B. Dehkordi, P. Neti, A.M Gole, and T.L. Maguire, "Development and Validation of a Comprehensive Synchronous Machine Model for a Real-Time Environment", *IEEE Trans. On Energy Conversion*, vol. 25, no.1, pp. 34-48, Mar 2010.
[4] A.B. Dehkordi, A.M Gole, and T.L. Maguire, "Permanent magnet synchronous machine model for real-time simulation", International Power System Transient Conference (IPST 2005), Montreal, June, 2005.
[5] B. R. Williams, W. R. Schmus, and D. C. Dawson, "Transmission voltage recovery delayed by stalled air conditioner compressors," *Power Systems, IEEE Transactions on*, vol. 7, no. 3, pp. 1173–1181, 1992.
[6] K. Prabakar, D. T. Rizy, F. Li, "A study on the effect of distribution circuit loading on air conditioner motor stall using a real time simulator," T&D Conference and Exposition, 2014 IEEE PES, April 2014.
[7] P.C. Krause, O.Wasynczuk, S.D. Sudhoff, Analysis of electric machinery, New York, IEEE Press, 1995.
[8] P. C. Krause, "Simulation of Unsymmetrical 2-Phase Induction Machines, " *IEEE Trans. Power Apparatus and Systems* , vol. PAS-84, No.11, pp. 1025-1037, Nov. 1965.
[9] S. D. Sudhoff, "Multiple Reference Frame Analysis of an Unsymmetrical Induction Machine, " *IEEE Trans. Energy Conversion*, vol. 8, No.3, pp. 425-432, Sep. 1993.
[10] P. Vas, Parameter, Parameter Estimation, Condition Monitoring, Diagnosis of Electrical Machines, Oxford Science. Publications, 1993.
[11] *RTDS User's Manual*, RTDS Technologies Inc., Winnipeg, Canada, 2014.
[12] H. W. Dommel, "Digital computer solution of electromagnetic transients in single and multiphase networks" ,IEEE Trans. Power Apparatus and Systems, vol.PAS-88, No.4, pp. 388-399, Apr. 1969.
[13] A.M. Gole, R.W. Menzies, D.A. Woodford and H. Turanli, "Improved interfacing of electrical machine models in electromagnetic transient programs," *IEEE Trans. Power Apparatus and Systems*, vol. PAS-103, no. 9, pp. 2446-2451, Sept. 1984.
[14] T.L. Maguire, "An Efficient Saturation Algorithm for Real Time Synchronous Machine Models using Flux Linkages as State Variables," Electrimacs 2002, Montreal, Canada, June 2002. *IEEE Trans. Power Apparatus and Systems*, vol. PAS-103, no. 9, pp. 2446-2451, Sept. 1984.
[15] G.R. Slemon, *Magnetoelectric devices*, New York, John Wiley &Sons, Inc., 1966, pp. 39-64.
[16] Sulzer Pumps, *Sulzer Centrifugal Pump Handbook*, Elsevier Advanced Technology, 1998, p. 62.

Ali B. Dehkordi (S'97, M'10) received the B.Sc. and M.Sc. degrees in electrical engineering from Sharif University of Technology, Tehran, Iran and Ph.D. degree from the University of Manitoba in 1999, 2002 and 2010 respectively. He worked as a research engineer for Sharif University of Technology in power quality projects in 2002. His research interests are on the modeling of power system components and in particular electric machines for Electromagnetic Transient Programs and Real Time Digital Simulation, the area that he has been working on for over 10 years. Dr. Dehkordi is a recipient of Dennis Woodford Prize, for "the most outstanding graduate thesis dealing with power system modeling and simulation". He is currently employed by RTDS Technologies Inc., Winnipeg, Canada.